Sub-threshold signal processing in arrays of non-identical nanostructures

2011 Nanotechnology 22 435201

(http://iopscience.iop.org/0957-4484/22/43/435201)

Nanotechnology **22** (2011) 435201 (9pp) doi:10.1088/0957-4484/22/43/435201

Sub-threshold signal processing in arrays of non-identical nanostructures

Javier Cervera, José A Manzanares and Salvador Mafé

Facultat de Física, Universitat de València, E-46100 Burjassot, Spain

E-mail: Javier.Cervera@uv.es

Received 13 May 2011, in final form 2 September 2011
Published 29 September 2011
Online at stacks.iop.org/Nano/22/435201

Abstract

Weak input signals are routinely processed by molecular-scaled biological networks composed of non-identical units that operate correctly in a noisy environment. In order to show that artificial nanostructures can mimic this behavior, we explore theoretically noise-assisted signal processing in arrays of metallic nanoparticles functionalized with organic ligands that act as tunneling junctions connecting the nanoparticle to the external electrodes. The electronic transfer through the nanostructure is based on the Coulomb blockade and tunneling effects. Because of the fabrication uncertainties, these nanostructures are expected to show a high variability in their physical characteristics and a diversity-induced static noise should be considered together with the dynamic noise caused by thermal fluctuations. This static noise originates from the hardware variability and produces fluctuations in the threshold potential of the individual nanoparticles arranged in a parallel array. The correlation between different input (potential) and output (current) signals in the array is analyzed as a function of temperature, applied voltage, and the variability in the electrical properties of the nanostructures. Extensive kinetic Monte Carlo simulations with nanostructures whose basic properties have been demonstrated experimentally show that variability can enhance the correlation, even for the case of weak signals and high variability, provided that the signal is processed by a sufficiently high number of nanostructures. Moderate redundancy permits us not only to minimize the adverse effects of the hardware variability but also to take advantage of the nanoparticles' threshold fluctuations to increase the detection range at low temperatures. This conclusion holds for the average behavior of a moderately large statistical ensemble of non-identical nanostructures processing different types of input signals and suggests that variability could be beneficial for signal processing. We demonstrate also that circuits composed of coupled non-identical nanoparticles can act as elementary nano-oscillators that show synchronization properties for sub-threshold stimuli. The results obtained should be of conceptual interest for the design of reliable signal processing schemes with non-identical nanostructures.

(Some figures in this article are in colour only in the electronic version)

1. Introduction

Non-linear dynamical systems can exploit noise to detect weak input signals [1–7]. Molecular-scaled biological networks [2, 3, 8, 9] composed of non-identical units which show some variability in their individual characteristics operate correctly in a noisy environment. The interplay between diversity and signal detection is crucial for neuronal sensory networks [2, 3], clusters of ion channels in cell membranes [8, 9], arrays of functionalized nanoparticles (NPs) [10], carbon nanotube [11] and nanowire [12] field-effect transistors, and nanoswitches based on a finite number of molecular dipoles [13].

Logical and signal processing based on nanostructures have attracted great interest due to the continuous miniaturization of electronics [14, 15]. For instance, the tunneling current through a gold colloid quantum dot between two electrodes could be modulated by the attached ligands, forming an NP-based single-electron transistor whose tunneling barriers consist of monolayers of thiols [16–22], although the nature of

the electrical contacts in the molecular junctions is also important [23]. We have considered theoretically the logics [24] and synchronization [25] of single-electron circuits whose building blocks are functionalized NPs. Electron tunneling in NPs is influenced by the discrete nature of charge transport and the Coulomb blockade (CB) energy barrier, which must be higher than the thermal energy for the transport of single electrons to be controlled [16, 18–21, 26]. The above condition is usually fulfilled by scaling down to the nanoscale where the problems of thermal noise and variability cannot be ignored. The variability acts as a static, diversity-induced noise that is added to the dynamic noise caused by thermal fluctuations [10, 11]. The high variability of individual nanostructures constitutes a serious issue for device design and application because of the fabrication uncertainties inherent to nanoscale experimental procedures. In particular, the size distribution of the metallic NPs [18–21, 27, 28] results in a significant spread of the individual threshold potentials. This experimental fact causes fluctuations in the threshold potential of the NPs that could not be ignored for voltage-driven applications [7–13].

The practical implementations of logical and signal processing schemes using nanostructures are expected to have a low reliability because of the weak signals involved, the thermal noise, and the variability. Fault-tolerant approaches [29, 30] are needed to carry out reliable information processing of weak signals using inherently unreliable components. Circuit redundancy has been proved as a feasible solution to the thermal noise and device variability problems [31]. We show here that redundancy not only solves the adverse effects of the hardware variability but also may turn this variability into an advantage. Variability can be beneficial provided that the signal is processed in parallel by a sufficiently high number of redundant nanostructures. Weak, sub-threshold signals can be reliably processed with a moderate increase in the number N of nanostructures because averaging enhances the system response.

Using kinetic Monte Carlo simulations, we explore theoretically the noise-assisted processing of sub-threshold signals using nanostructures whose basic properties have been shown experimentally [18–21, 27]. In particular, we consider arrays of metallic NPs functionalized with organic ligands that act as tunneling junctions connecting the NP to the external electrodes [16–20]. The correlation between different input (potential) and output (current) signals is studied as a function of the signal strength, temperature, variability, and the circuit redundancy. We demonstrate significant enhancement of the input–output correlation in the signal processing by NPs that show a high variability in the threshold potentials. Moreover, redundancy takes advantage of this variability to increase the detection range at low temperatures. Finally, we prove that resistively coupled arrays of non-identical structures can act as nano-oscillators that show collective signal processing and synchronization properties. While the main emphasis is on the reliability of the signal processing using these nanostructures, the results may also be relevant to neuronal sensory networks where variability is important for information processing and synchronization phenomena [2–6].

2. Model and simulation procedure

Figure 1(a) shows an elementary nanostructure formed by a metallic NP linked to two electrodes by organic ligands. A potential V is applied to the left electrode with respect to the right one. The left and right ligands act as tunneling junctions with capacitances C_L and C_R and tunneling resistances R_L and R_R much higher than the quantum resistance $R_0 = h/e^2 = 26\ \mathrm{k\Omega}$, where e is the elementary charge and h is Planck's constant. This condition confines the electrons within the NP. We can neglect the existence of discrete quantum electronic energy levels because of the relatively high NP volume [18–20]. The transport of electrons across the nanostructure occurs then by tunneling and is dominated by the CB effect. At absolute zero temperature, electron transport from the negative electrode to the (uncharged) NP can only occur when the applied voltage $|V|$ is higher than the threshold potential $V_{th} = e/C_\Sigma$, where $C_\Sigma = C_L + C_R$ is the total capacitance. For the sake of simplicity, we consider $C_L = C_R$. At finite temperatures, according to the orthodox theory, the electron transfer rates are [10, 24, 26]

$$\Gamma_L^{\rightleftarrows} = \frac{1}{eR_L^2}\frac{-\Delta E_L^{\rightleftarrows}}{1-\exp(\Delta_L^{\rightleftarrows}/kT)} \tag{1}$$

$$\Gamma_R^{\rightleftarrows} = \frac{1}{eR_R^2}\frac{-\Delta E_R^{\rightleftarrows}}{1-\exp(\Delta_R^{\rightleftarrows}/kT)} \tag{2}$$

where k is Boltzmann's constant, T is the absolute temperature, and

$$\Delta E_L^{\rightleftarrows} = \pm\frac{e^2}{C_\Sigma}\left[\frac{1}{2}+n+\frac{C_R V}{e}\right] = \pm\frac{e}{2}V_{th}(1+2n)+V \tag{3}$$

are the changes in the electrostatic energy when the electron is transferred from the left electrode to the NP ($\rightarrow$) and from the NP to the left electrode ($\leftarrow$), n is the electronic occupancy of the NP (the excess or defect number of electrons). Similarly,

$$\Delta E_R^{\rightleftarrows} = \mp\frac{e^2}{C_\Sigma}\left[\frac{1}{2}+n-\frac{C_L V}{e}\right] = \mp\frac{e}{2}V_{th}(1+2n)-V \tag{4}$$

are the energy changes when the electron is transferred from the NP to the right electrode ($\rightarrow$) and from the right electrode to the NP ($\leftarrow$). For $n = 0$ and $V > 0$, positive values of the signal-to-threshold distance $V_{th} - V$ correspond to the sub-threshold potentials characteristic of weak signals while negative values correspond to supra-threshold potentials.

The calculated current–voltage curve of figure 1(b) shows the typical trends found experimentally [20, 21, 27]. The electrostatic energy diagram is shown in figure 1(c) for $n = 0$ and a sub-threshold potential $0 < V < V_{th}$. The height of the energy barrier is $\Delta E_L^{\rightarrow} = e(V_{th}+V)/2 > 0$, as seen from the L electrode, and $\Delta E_R^{\leftarrow} = e(V_{th}-V)/2 > 0$, as seen from the R electrode. At low temperatures, $kT/e \ll V_{th}$, the transfer rate from the right electrode to the NP is non-zero even at sub-threshold voltages ($0 < V < V_{th}$, $\Delta E_R^{\leftarrow} > 0$) but it is only significant for supra-threshold voltages ($0 < V_{th} < V$, $\Delta E_R^{\leftarrow} < 0$). The transfer rates increase with the thermal

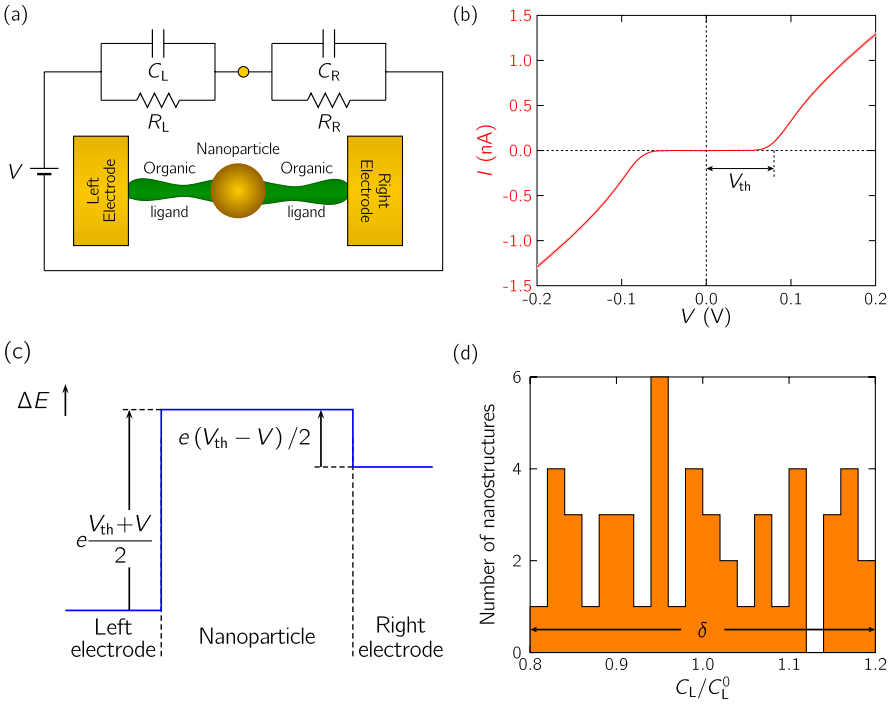

Figure 1. (a) Scheme of the nanostructure composed of a metallic NP linked to the electrodes by organic ligands acting as tunneling junctions and the equivalent electrical circuit. (b) The current–voltage curve of the nanostructure together with the noise amplitude (shaded region). The electrical parameters of the nanostructure are $C_L = C_R = 1$ aF and $R_L = R_R = 50$ MΩ, and the temperature is $T = 30$ K. At low temperatures, the current is negligible for $V < V_{th} = e/(C_L + C_R) = 80$ mV because of the CB effect. (c) The electrostatic energy diagram of the electron for a sub-threshold voltage V in the case $C_L = C_R$. (d) A randomly generated distribution of the individual left capacitances of $N = 50$ nanostructures with a relative variability $\delta = 0.4$. It is this variability that causes a distribution of threshold potentials, giving different energy diagrams for each nanostructure (see (c)).

energy kT and give a fluctuating current with a characteristic thermal noise (see figure 1(b)).

We analyze the processing of a weak, sub-threshold input signal $V(t)$ using a parallel array of N nanostructures similar to that of figure 1(a). The output is the current $I_i(t)$ through nanostructure i. However, because the currents generated by weak signals are small, their fluctuations should also be considered when analyzing the signal processing reliability. The signal processing is based on the fact that, at finite temperatures, the output shows a positive correlation with the input, even for sub-threshold input signals. A kinetic Monte Carlo method is used to simulate the transport of electrons through the parallel array of nanostructures [10]. In every simulation step, the potential and occupation state of every NP are changed and this modifies the transfer rates according to equations (1)–(4). In the time interval from t to $t + \Delta t$, the current through nanostructure i is calculated from the charge ΔQ_i transported by the net number of electrons transferred, $I_i(t) = \Delta Q_i/\Delta t$, with $\Delta t = 1$ μs.

Ligand-stabilized metallic NPs a few nanometers in radii have effective capacitances of the order of 10^{-18} F = 1 aF. The CB effect appears then at sub-ambient and close to ambient temperatures [12, 16, 17, 21]. In fact, electrochemical Coulomb staircases have been observed in room-temperature solutions of NPs with approximately monodisperse cores because of their sub-attofarad double layer capacitances [18]. However, fabrication procedures give structures with a high variability in their physical properties. This experimental fact leads to statistical distributions for the values of the electrical parameters in the equivalent circuit of figure 1(a), as is shown schematically in figure 1(d) [28] (see also [31] and references therein). Eventually, these distributions must give different threshold potentials $V_{th,i}$ for the different NPs. Therefore, each NP has a different current I_i under the same applied potential V. At low temperature, those NPs characterized by $V_{th,i} > V$ show a very small current because of the CB effect. To study the effect of variability on the signal processing, we have considered a set of N non-identical structures whose electrical parameters C_L, C_R, R_L, R_R have a random distribution of values with a maximum variability. For instance, the capacitances $C_{L,i}$ ($1 \leqslant i \leqslant N$) are distributed randomly around a central value C_L^0 with a maximum relative variability δ, so that

$$1 - \frac{\delta}{2} \leqslant \frac{C_{L,i}}{C_L^0} \leqslant 1 + \frac{\delta}{2}. \tag{5}$$

In the results of sections 3.1 and 3.2 below, we use $C_L^0 = C_R^0 = 1$ aF and $R_L^0 = R_R^0 = 50$ MΩ as typical electrical parameters for metallic NPs with ligand shells [4, 5, 10, 18–20, 24, 25]. The central threshold potential is $V_{th}^0 = e/C_\Sigma^0 \approx 80$ mV and the individual threshold potentials $V_{th,i}$ vary from 64 to 107 mV when $\delta = 0.5$.

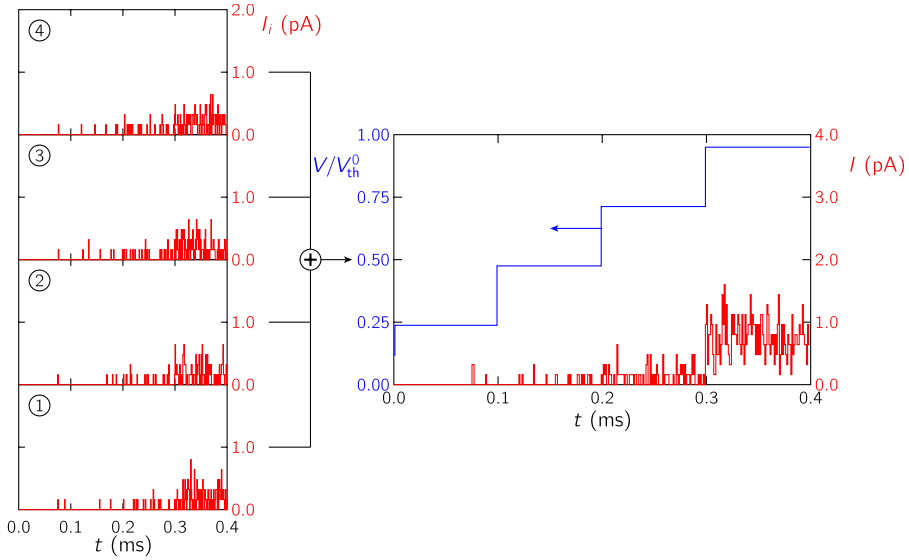

Figure 2. The individual (I_i) and total (I) currents (in red) at 30 K for a parallel array of four identical nanostructures ($\delta = 0$, no variability) when a sub-threshold multi-step potential (in blue) is applied to the electrodes.

3. Results and discussion

3.1. Sub-threshold signal processing enhancement

Figure 1(b) shows that the I–V curve of a nanostructure is highly non-linear in the vicinity of the threshold potential. NPs with different threshold potentials have then very different currents under the same applied potential, within the non-linear behavior range. The NPs with smaller threshold potentials show higher currents and those with larger threshold potential show lower currents. Because of the non-linearity of the I–V curve the former have a larger influence on the total current. If the circuit redundancy (i.e. the number of nanostructures in the parallel array) is large enough, the presence of some nanostructures with high output current, and hence a large total current, is ensured. This large total current implies a better correlation with the input potential signal and improves the signal processing reliability. We show next that the variability can improve the signal processing even for a moderate circuit redundancy.

Figures 2 and 3 show the output currents I_i of four nanostructures at 30 K with an applied multi-step potential

$$V(t) = V_0[H(t) + H(t-\tau) + H(t-2\tau) + H(t-3\tau)] \quad (6)$$

where $H(t)$ is the Heaviside step function, $V_0 = 0.95V_{th}^0/4$ and $\tau = 100\ \mu$s. The total current $I(t)$ resulting from the sum of the individual currents I_i and the potential $V(t)$, scaled to the central threshold potential $V_{th}^0 = 80$ mV, are also shown. The minor differences in the currents of the four identical nanostructures of figure 2 ($\delta = 0$) are due to the thermal noise. The large differences in the currents of the non-identical nanostructures of figure 3 are due to both the thermal noise and the variability ($\delta = 0.5$). In this particular case, the randomly generated electrical parameters of the nanostructures have resulted in threshold potentials between $V_{th,3} = 71.6$ mV and $V_{th,2} = 85.7$ mV. At 30 K, the thermal potential kT/e and the potential barrier $V_{th}^0 - V$ are both in the 1–10 mV range and then the thermal energy is high enough to overcome some of the individual threshold potentials, which explains the different behavior observed in figures 2 and 3.

In figure 3, the output of nanostructure 2 is very small but nanostructure 3 has an output higher than that observed for every nanostructure of figure 2. Hence, the correlation between $V(t)$ and some of the individual currents $I_i(t)$ in figure 3 is lower than in figure 2. This result might lead to the (wrong) conclusion that the reliability of the signal processing worsens due to their variability. Contrarily, when $V(t)$ and the total current $I(t)$ are considered, figures 2 and 3 show that the variability enhances the correlation. The current through nanostructure 3 in figure 3 is so high that its contribution to the total current compensates for the low current through nanostructure 2.

Variability effects can be observed at higher temperatures in systems with potential barriers in the 10–100 mV range because $kT/e = 26$ mV at ambient temperature. This case has recently been demonstrated for field-effect nanowire transistors with different individual characteristics [12]. The experimental variability resulted in a distribution of multi-threshold potentials for the nanowires (see figures 1 and 4 in [12]). The theoretical results of figure 3 agree qualitatively with the experimental results of figure 4(b) in [12] for the electric current through the nanowires, thus confirming that variability can be beneficial for signal processing.

3.2. Statistical analysis of the signal processing enhancement

In this section the output currents are calculated as average values from 100 simulations. This large number of simulations is chosen to gather meaningful statistics. In every kinetic Monte Carlo simulation a new sample of the parallel array is prepared by changing the values of the electrical parameters of the N nanostructures according to a random distribution

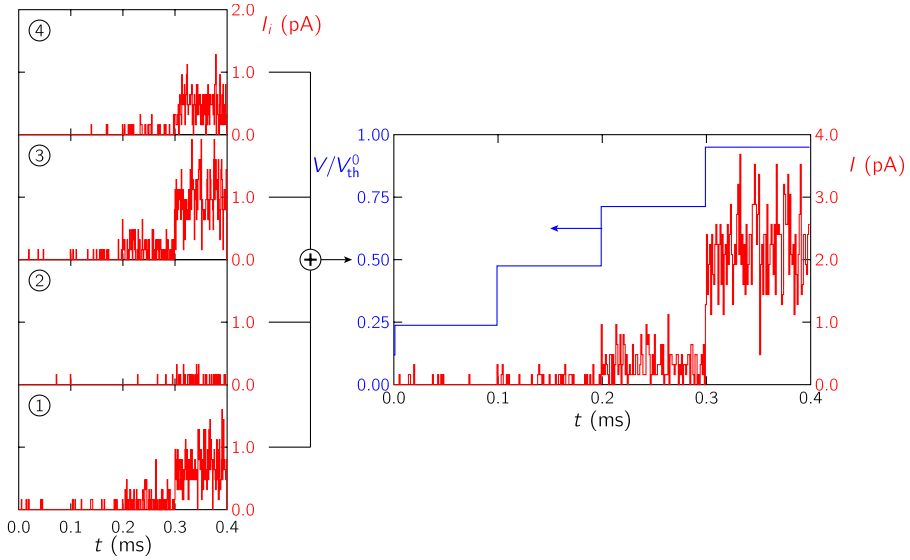

Figure 3. The individual (I_i) and total (I) currents (in red) at 30 K in a parallel array of four different nanostructures ($\delta = 0.5$) when a sub-threshold multi-step potential (in blue) is applied to the electrodes.

with maximum relative variability δ. Different output currents are obtained in each simulation because of the variability and thermal noise effects. If I_{max} and I_{min} denote the maximum and minimum values observed, respectively, the current fluctuation is estimated as $\varepsilon(I) = (I_{max} - I_{min})/2$. Most calculated current lies within the interval $\langle I \rangle \pm \varepsilon(I)$, shown in the plots as error bars or shadow regions, where $\langle I \rangle$ is the average value of the currents obtained in 100 simulations. In a parallel array of different nanostructures, the individual threshold potentials $V_{th,i}$ show some variability. The maximum total current I_{max} is observed when most of the NPs have low threshold potentials $V_{th,i} \approx V_{th}^0/(1 + \delta/2)$ and the minimum total current I_{min} is observed when most of the NPs have high threshold potentials $V_{th,i} \approx V_{th}^0/(1 - \delta/2)$.

Obviously, the current fluctuation $\varepsilon(I)$ increases with the variability because the diversity-induced noise adds to the thermal noise. However, the variability effect on the average current $\langle I \rangle$ is not so predictable. Figures 2 and 3 have shown that one particular parallel array of non-identical nanostructures can have a larger total current than a similar array of identical nanostructures. In the following paragraphs we demonstrate that this conclusion holds for most arrays of non-identical nanostructures and, particularly, for the average behavior of a large statistical ensemble of non-identical nanostructures. Moreover, we show that its validity is not restricted to the multi-step input potential considered in figures 2 and 3 but it is also confirmed for other types of input signals.

Figure 4 shows the total current $I(t)$ at 30 K for $N = 50$ and the sinusoidal input potential $V = V_0 \sin(2\pi t/\tau)$, with $\tau = 100$ μs. The results correspond to the average currents $\langle I \rangle$ (dashed line for $\delta = 0$ and solid line for $\delta = 0.5$) and the shadow regions indicate their fluctuations $\varepsilon(I)$. Figure 4(a) evidences that the total current is significantly higher for $\delta = 0.5$ than for $\delta = 0$ in the case of a sub-threshold signal of amplitude $V_0 = 0.6V_{th}^0$. Because the

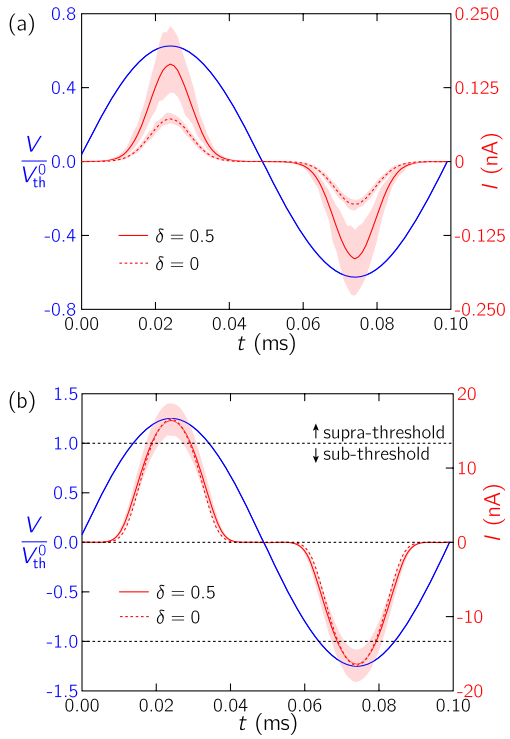

Figure 4. The total current $I(t)$ (right axis) at 30 K for a parallel array of $N = 50$ nanostructures when a sinusoidal potential (left axis) of amplitudes $V_0 = 0.6V_{th}^0$ (a) and $V_0 = 1.2V_{th}^0$ (b) is applied to the electrodes. The average current is obtained from 100 simulations for $\delta = 0$ (dashed line) and $\delta = 0.5$ (solid line). The current fluctuation is shown by the shadow regions and it is very small in the case of $V_0 = 1.2V_{th}^0$ and $\delta = 0$ because of the low temperature.

current through an individual nanostructure increases non-linearly with potential for values close to its threshold potential (see figure 1(b)), the contribution to the total current of a small fraction of nanostructures with $V_{th,i} < V_{th}^0$ can be so large that

it compensates for the small contribution of a large fraction of NPs with $V_{\mathrm{th},i} > V_{\mathrm{th}}^0$. This compensation occurs when the variability δ and the redundancy N are high enough to ensure a significant number of NPs with low threshold potentials and, hence, an increased total current. The correlation between the input and output signals for the case of sub-threshold potentials is then enhanced because of the variability.

Figure 4(b) considers the case of a supra-threshold signal of amplitude $V_0 = 1.2V_{\mathrm{th}}^0$. Compared to figure 4(a), 4(b) shows a dramatic increase by two orders of magnitude in the total current because of the non-linearity of the system: the current at $0.6V_{\mathrm{th}}^0$ in figure 4(b) is as low as that of figure 4(a) and currents in the nanoampere regime are only obtained for potentials higher than $0.8V_{\mathrm{th}}^0$. For the same reasons explained above, the average current is larger for $\delta = 0.5$ than for $\delta = 0$; however, this current enhancement is small for supra-threshold potentials (compare figure 4(a) to (b)) and the main effect of variability is an increase of the current fluctuation. The absence of a significant current enhancement is associated with the loss of the non-linearity in the current–voltage: the change of the current with the potential is approximately linear for supra-threshold potentials (see figure 1(b)). The variability of individual threshold potentials still results in a range of individual output currents but the average current is then determined by the central threshold potential.

Figures 3 and 4 show that the processing of weak signals could be enhanced by the combined effects of the thermal noise and the diversity-induced noise. Thermal energy allows the electrons to go through the nanostructure and the variability improves the system response because of the diversity of threshold potentials. This enhancement is reminiscent of the result obtained for networks of model neurons subject to different individual noises [2, 3, 6] (compare figure 2 of [2] to figures 3 and 4 here) and model systems composed of coupled units with significant threshold variability driven by an external periodic signal [32]. In these cases, an appropriate level of variability can improve the system response to the input signal and this result leads us to speculate that the variability observed in some biological systems may have an important function [32]. Structural variability also plays a constructive role in the detection of sub-threshold extracellular signals [33] as well as in opinion-formation models with individuals that have diverse preferences and opinions [34]. This diversity-induced resonance causes external influences such as advertising to be better followed by populations with a suitable level of diversity in their preferences, rather than by other populations with identical or too differing individuals [32, 34].

Figure 5(a) shows the total root mean square current $I_{\mathrm{rms}} = \sqrt{\langle I^2 \rangle}$ at 30 K of a parallel array with $N = 50$ as a function of the amplitude V_0 of the input potential

$$V(t) = \begin{cases} V_0, & 0 < t < \tau/2 \\ -V_0, & \tau/2 < t < \tau \end{cases} \qquad (7)$$

where $\tau = 100\ \mu$s. In the case of identical nanostructures ($\delta = 0$), the results in figure 5(a) are qualitatively similar to those of figure 1(b) because every nanostructure has the same contribution to the total current. The current is negligible when $V_0 \ll V_{\mathrm{th}}^0 = 80$ mV, becomes significant when V_0 is close to V_{th}^0, and increases almost linearly with V_0 for higher values of V_0. These general trends are also observed in the array of non-identical nanostructures ($\delta = 0.5$), but there are significant quantitative differences. The inset of figure 5(a) clearly shows an enhancement of the total current because of the variability. The ratio of the currents obtained for $\delta = 0.5$ and 0 has a maximum when V_0 is about $V_{\mathrm{th}}^0/2 = 40$ mV and tends to unity when V_0 exceeds V_{th}^0 because the I–V curve of the individual nanostructures is practically linear in the $V_0 > V_{\mathrm{th},i}$ regime. These results confirm the observations made in figures 4(a) and (b), suggesting that the main conclusions are not affected by the particular input signal considered.

Figures 5(b) and (c) show how temperature modifies the influence of variability on the total current, and hence on the reliability of the processing of a sub-threshold signal. The rms current increases with the temperature. Since $V_0 = 50$ mV and $V_{\mathrm{th}}^0 \approx 80$ mV, the CB prevents the transport of electrons at low temperatures and the current is very low until the thermal energy kT is high enough to increase the tunneling rates. In this temperature range, the variability effects are significant (see figure 5(c) and the inset of figure 5(b)). At high temperatures, however, the current is high (because the potential barrier becomes similar to kT/e) and its average value becomes independent of the variability δ (see figure 5(c)). For the temperature range in figure 5(c), the contribution of the variability to the current fluctuation is larger than that due to thermal noise and this fluctuation increases with the variability (compare the error bars for $\delta = 0.5$ and 0.3). Because the variability is kept constant and $\sqrt{\langle I^2 \rangle}$ increases with temperature, there is a decrease in the uncertainty of the ratio $\sqrt{\langle I^2 \rangle(\delta)/\langle I^2 \rangle(0)}$ with temperature.

The current enhancement due to the variability observed in figures 5(a) (inset) and (c) is possible because of the redundancy. In a parallel array of non-identical nanostructures, the variability can increase the total current if redundancy allows for some NPs with so low threshold potentials that their large contribution to the total current compensates for the small contribution of other nanostructures. Figure 5(d) shows the current per nanostructure $\sqrt{\langle I^2 \rangle}/N$ at 30 K as a function of the number of nanostructures for $\delta = 0.5$ and $V_0 = 50$ mV. The average value of $\sqrt{\langle I^2 \rangle}/N$ is practically constant but its uncertainty decreases with increasing N. The increase in the number of nanostructures (system redundancy) improves the performance of the system: weak, sub-threshold signals can be processed with a moderate increase in N because averaging enhances the system response. Variability can then enhance the system response provided that the signal is processed by a sufficiently high number of redundant nanostructures.

3.3. Synchronization of NP potential oscillations

Figure 6(a) shows a resistance-single electron transistor (R-SET) nanostructure composed of a metallic NP of capacitance C_i connected to the right electrode by a tunneling junction of resistance R_i and to the left electrode by an effective charging resistance r_i. If the potential $V > 0$ applied to the left electrode

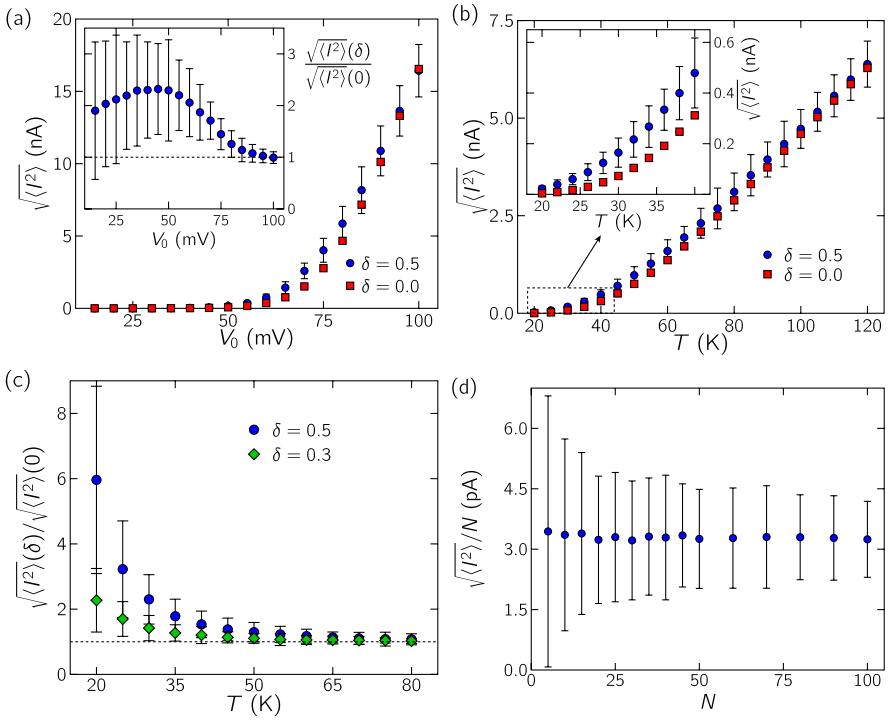

Figure 5. (a) $\sqrt{\langle I^2\rangle}$ as a function of the potential amplitude V_0 of the potential in equation (7) at 30 K for the cases $\delta = 0.5$ and 0 (the current fluctuation is very small for $\delta = 0$ because of the low temperature). The inset shows the ratio of $\sqrt{\langle I^2\rangle}$ for the two variabilities. (b) $\sqrt{\langle I^2\rangle}$ as a function of the temperature for $\delta = 0.5$ and 0 at $V_0 = 50$ mV. The inset zooms the low temperature region. (c) The ratio $\sqrt{\langle I^2\rangle(\delta)/\langle I^2\rangle(0)}$ as a function of temperature for $\delta = 0.3$ and 0.5 at $V_0 = 50$ mV. (d) $\sqrt{\langle I^2\rangle}/N$ as a function of the number of nanostructures N for $V_0 = 50$ mV, $T = 30$ K, and $\delta = 0.5$.

exceeds a threshold value $V_{\rm th} = e/(2C)$, the NP potential $V_i(t)$ exhibits an oscillatory behavior associated with the charging–tunneling process and the CB effect at low temperatures. When $r_i \gg R_i$, $V_i(t)$ increases due to the charging process described by the differential equation

$$C\frac{{\rm d}V_i}{{\rm d}t} = \frac{V - V_i}{r_i}. \tag{8}$$

Because of the discreteness of the charge, the NP charging should occur in a multi-step process but the fact is that a continuum approach captures the basic characteristics of the problem [25]. This approach is valid when the number of elementary steps is sufficiently high so that the charging time is approximately constant. The electron tunneling rate between the right electrode and the NP is described by equations (2) and (4). A tunneling event produces a change in the NP potential equal to $-2V_{\rm th}$ if the electron tunnels from the right electrode and is equal to $+2V_{\rm th}$ if the electron tunnels from the NP to the right electrode. In the simulation of this charging–tunneling process, $V_i(t)$ is changed at every time step because of the charging and the possibility of electron tunneling is evaluated.

A number N of different R-SET nanostructures can be connected in a parallel array and coupled using a common resistance $r_{\rm S}$ (see figure 6(b)). This coupling causes every nanostructure to be affected by the state of the others and produces synchronization phenomena [25, 35]. The addition of the resistance $r_{\rm S}$ couples the individual charging processes so that the charging rate $C_i\,{\rm d}V_i/{\rm d}t$ of the ith NP depends on the charging rates $C_j\,{\rm d}V_j/{\rm d}t$ of the other NPs in the array according to the equation

$$(r_i + r_{\rm S})C_i\frac{{\rm d}V_i}{{\rm d}t} + r_{\rm S}\sum_{j\neq i}^{N} C_j\frac{{\rm d}V_j}{{\rm d}t} = V - V_i. \tag{9}$$

The coupling strength is characterized by the dimensionless parameter [25]

$$K_{\rm C} \equiv r_{\rm S}\sum_{i=1}^{N} 1/r_i. \tag{10}$$

For the system of figure 6(b), we consider that an input weak potential signal is detected if it produces synchronized potential oscillations. For a system of identical nanostructures ($\delta = 0$) at 5 K, the oscillations are only observed when the applied potential V is higher than their threshold potential. However, when $\delta > 0$ some of the NPs have low threshold potentials $V_{{\rm th},i} < V_{\rm th}^0$ and start oscillating when the applied potential is in the range $V_{{\rm th},i} < V < V_{\rm th}^0$. Because the nanostructures of figure 6(b) are strongly coupled, the oscillation of a small fraction of NPs with low threshold potentials causes the potentials of the other NPs to oscillate with the same frequency and phase.

The synchronization is first illustrated in figure 6(c) for a parallel array of $N = 3$ at 5 K with the electrical parameters $V_0 = 100$ mV, $r_1 = 1.08$ GΩ, $r_2 = 0.97$ GΩ, $r_3 = 1.02$ GΩ, $R_1 = 37.7$ MΩ, $R_2 = 45.8$ MΩ, $R_3 = 45.7$ MΩ, $C_1 =$

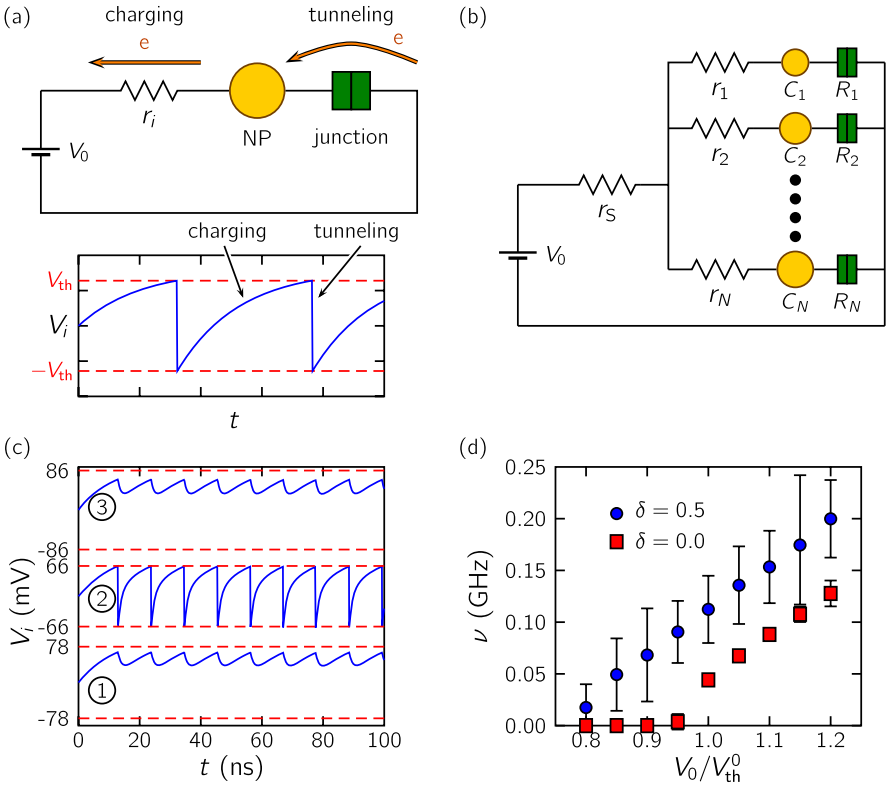

Figure 6. (a) Scheme of a resistance-single electron transistor (R-SET) formed by an NP linked to the electrodes by a tunneling junction of resistance R_i and a charging resistance r_i. If $R_i \ll r_i$, an oscillatory charge-tunneling process occurs at low temperatures. (b) Using a common resistance r_S, it is possible to couple the individual electrical states of N nanostructures in a parallel array. (c) When the coupling is sufficiently high, the potential oscillations become synchronized with the same frequency and phase. The results correspond to the individual time recordings of the potentials for three NPs at $K_C = 10$ and 5 K. (d) Frequency ν of the synchronized oscillations for $N = 10$ nanostructures with a coupling constant $K_C = 10$ as a function of the applied potential in the cases $\delta = 0$ and 0.5.

1.03 aF, $C_2 = 1.21$ aF, $C_3 = 0.93$ aF, and $r_S = 3.41$ GΩ, which give the threshold potentials indicated in the figure. These results have been obtained using a mixed continuum Monte Carlo approach [25]. In the absence of coupling, the individual potential oscillations would occur at different frequencies because of the different time constants $r_i C_i$. In the presence of coupling, the potential jump from V_{th} to $-V_{th}$ in one NP due to tunneling affects the potentials of the other two NPs. For high enough K_C, the nanostructures are strongly coupled and the three NP potentials become synchronized (i.e. the NP potentials oscillate with the same frequency and phase) as shown in figure 6(c). Qualitatively similar results have recently been obtained for neuromorphic, single-electron circuits based on integrate and fire neuronal units that were simulated at lower temperatures and variability values than those considered here [36]. These circuits show pulse-density modulation when the output is fed back to all the oscillators through a capacitive coupling [5, 36] instead of the resistive coupling of figure 6(b).

Figure 6(d) shows the synchronized oscillation frequency of $N = 10$ strongly coupled nanostructures ($K_C = 10$) at 5 K as a function of the applied potential V. For every point, 100 simulations have been carried out and each simulation runs for a system time of about 200 ns. In the simulations the electrical parameters r_i, R_i and C_i of the different nanostructures have been changed according to a random distribution of central values $r^0 = 1$ GΩ, $R^0 = 50$ MΩ, $C^0 = 1$ aF, and relative variability δ. The average values of the oscillation frequency are indicated by the circles ($\delta = 0.5$) and squares ($\delta = 0$) and their uncertainties by the error bars in figure 6(d). These uncertainties originate from the thermal noise (note that tunneling can occur for $V < V_{th}^0$ at finite temperature) and, especially, from the variability (note that a different sample of the system with different threshold potentials is used in every simulation). The results of figure 6(d) show that variability helps to increase the detection range of the system. In particular, figure 6(d) shows that synchronized, collective oscillations are observed only for $V > 0.94 V_{th}^0$ approximately when $\delta = 0$ while lower applied potentials already trigger the collective oscillations in the case $\delta = 0.5$. Once the potential oscillations start, increasing further the potential increases the charging currents and, hence, the oscillation frequencies.

The synchronization of potential oscillations described above is reminiscent of that found in networks of non-identical neurons [2, 3, 36] and shows clearly that the variability can be beneficial not only to extend the range of signal processing but also to enhance the cooperative response of the system. This remarkable collective property is based on: (i) a finite distribution of individual threshold potentials that is available for the first NP oscillation to start and (ii) the strong coupling making it possible that NPs with low threshold potentials force the other NPs with high threshold potentials

to oscillate with the same frequency and phase. Cooperative phenomena are characteristic of biological networks and could also be exploited in redundant molecular circuits composed of many units that are not identical because of the fabrication uncertainties inherent to the nanoscale.

4. Conclusions

Weak input signals are routinely processed by molecular-scaled biological networks composed of significantly different basic units that can operate correctly in a noisy environment [2, 3, 8, 9, 33]. It is worth reconsidering this question on the basis of more simplified molecular systems amenable to fundamental physical analysis. This is the case of arrays of metallic NPs functionalized with organic ligands acting as tunneling junctions. These arrays constitute a simple idealization of nanoscale circuits whose building blocks are based on the CB and tunneling effects. Practical implementations of logical and signal processing schemes with these nanostructures are difficult not only because of the interconnections but also because of the low system reliability caused by the weak signals involved, the thermal noise, and the variability. We have conducted extensive kinetic Monte Carlo simulations to study the correlation between the input (potential) and the output (current) signals, as well as the absolute value of the current and its fluctuations, as a function of temperature, applied voltage, and number of nanostructures. The results show that variability can enhance the correlation, even for the case of weak signals and high variability, provided that the signal is processed by a sufficiently high number of nanostructures. Moderate redundancy permits us not only to minimize the adverse effects of the hardware variability but also to take advantage of the nanoparticles' threshold fluctuations to increase the detection range at low temperatures. This conclusion holds for the average behavior of a moderately large statistical ensemble of non-identical nanostructures processing different types of input signals and suggests that variability could be beneficial for signal processing. Remarkably, similar results have been demonstrated experimentally for ion channels in cell membranes [8, 9] and carbon nanotube [11] and nanowire [12] field-effect transistors showing significant variability, which supports the validity of the present concepts for the design of reliable signal processing schemes with many non-identical nanostructures. Finally, we demonstrate that circuits composed of coupled non-identical nanoparticles can act as elementary nano-oscillators that show synchronization properties for sub-threshold stimuli.

Acknowledgment

Financial support from the Ministry of Science and Innovation of Spain (project MAT2009-07747) is acknowledged.

References

[1] Gammaitoni L, Hanggi P, Jung P and Marchesoni F 1998 *Rev. Mod. Phys.* **70** 1
[2] Stein R B, Gossen E R and Jones K E 2005 *Nature Rev. Neurosci.* **6** 389
[3] White J A, Rubinstein J T and Kay A R 2000 *Trends Neurosci.* **23** 131
[4] Oya T, Asai T and Amemiya Y 2007 *Chaos Solitons Fractals* **32** 855
[5] Oya T, Asai T, Kagaya R, Kasai S and Amemiya Y 2006 *Int. Congr. Ser.* **129** 213
[6] Collins J J, Chow C C and Imhoff T T 1995 *Nature* **376** 236
[7] Kasai S and Asai T 2008 *Appl. Phys. Express* **1** 083001
[8] Rubinstein J T 1995 *Biophys. J.* **68** 779
[9] Barber M J and Ristig M L 2006 *Phys. Rev.* E **74** 041913
[10] Cervera J, Manzanares J A and Mafé S 2010 *Nanoscale* **2** 1033
[11] Hakamata Y, Ohno Y, Maehashi K, Kasai S, Inoue K and Matsumoto K 2010 *J. Appl. Phys.* **108** 104313
[12] Kasai S, Miura K and Shiratori Y 2010 *Appl. Phys. Lett.* **96** 194102
[13] Mafé S, Manzanares J A and Reiss H 2011 *J. Appl. Phys.* **109** 044302
[14] Blencowe M P 2007 *Contemp. Phys.* **46** 249
[15] Ray V, Subramanian R, Bhadrachalam P, Ma L-C, Kim C-U and Koh S J 2008 *Nature Nanotechnol.* **3** 603
[16] Garcia-Morales V and Mafé S 2007 *J. Phys. Chem.* C **111** 7242
[17] Brust M, Walker M, Bethell D, Schifrin D and Whyman R 1994 *J. Chem. Soc. Chem. Commun.* 801
[18] Chen S, Ingram R S, Hostetler M J, Pietron J J, Murray R W, Schaaff T G, Khoury J T, Alvarez M M and Whetten R L 1998 *Science* **280** 2098
[19] Quinn B M, Liljeroth P, Ruiz V, Laaksonen T and Kontturi K 2003 *J. Am. Chem. Soc.* **125** 6644
[20] Chaki N K, Kakade B, Vijayamohanan K P, Singh P and Dharmadhikari C V 2006 *Phys. Chem. Chem. Phys.* **8** 1837
[21] Brousseau L C III, Zhao Q, Shultz D A and Feldheim D L 1998 *J. Am. Chem. Soc.* **120** 7645
[22] Wang W, Lee T and Reed M A 2003 *Phys. Rev.* B **68** 035416
[23] Akkerman H B and de Boer B 2008 *J. Phys.: Condens. Matter* **20** 013001
[24] Cervera J and Mafé S 2010 *ChemPhysChem* **11** 1654
[25] Cervera J, Manzanares J A and Mafé S 2009 *J. Appl. Phys.* **105** 074315
[26] Likharev K 1999 *Proc. IEEE* **87** 606
[27] Kano S, Azuma Y, Kanehara M, Teranishi T and Majima Y 2010 *Appl. Phys. Express* **3** 105003
[28] Wang Z T B, Hussain I, Schaeffer N, Wyatt M F, Brust M and Cooper A I 2007 *Langmuir* **23** 885
[29] Nikolic K, Sadek A and Forshaw M 2002 *Nanotechnology* **13** 357
[30] Martorell F and Rubio A 2009 *Microelectron. J.* **39** 1041
[31] Cervera J, Manzanares J A and Mafé S 2009 *Nanotechnology* **20** 465202
[32] Chen H, Hou Z and Xin H 2009 *Physica* A **388** 2299
[33] Chen H S, Zhang J Q and Liu J Q 2007 *Phys. Rev.* E **75** 041910
[34] Tessone C J and Toral R 2009 *Eur. Phys. J.* B **71** 549
[35] Strogatz S H 1994 *Non-linear Dynamics and Chaos: with Applications to Physics, Biology, Chemistry, and Engineering* (Cambridge: Perseus books)
[36] Kikombo A K, Asai T, Oya T, Schmid A, Leblebici Y and Amemiya Y 2009 *Int. J. Nanotechnol. Mol. Comput.* **1** 80